Journal of Solid State Chemistry 183 (2010) 2511–2515

Contents lists available at ScienceDirect

Journal of Solid State Chemistry

journal homepage: www.elsevier.com/locate/jssc

Mesoporous mixed metal oxides derived from P123-templated Mg–Al layered double hydroxides

Jun Wang [a,b,c,*], Jideng Zhou [a], Zhanshuang Li [a], Yang He [a], Shuangshuang Lin [a], Qi Liu [a], Milin Zhang [a,c], Zhaohua Jiang [b]

[a] College of Material Science and Chemical Engineering, Harbin Engineering University, Harbin 150001, PR China
[b] College of Chemical Engineering, Harbin Institute of Technology, Harbin 150001, PR China
[c] The Key Laboratory of Superlight Materials and Surface Technology, Ministry of Education, 150001, PR China

ARTICLE INFO

Article history:
Received 25 May 2010
Received in revised form
16 August 2010
Accepted 19 August 2010
Available online 24 August 2010

Keywords:
Mesoporous
Mixed metal oxides
Layered double hydroxides
Pluronic P123

ABSTRACT

We report the preparation of mesoporous mixed metal oxides (MMOs) through a soft template method. Different amounts of P123 were used as structure directing agent to synthesize P123-templated Mg–Al layered double hydroxides (LDHs). After calcination of as-synthesized LDHs at 500 °C, the ordered mesopores were obtained by removal of P123. The mesoporous Mg–Al MMOs fabricated by using 2 wt% P123 exhibited a high specific surface area of 108.1 m^2/g, and wide distribution of pore size (2–18 nm). An investigation of the "memory effect" of the mesoporous MMOs revealed that they were successfully reconstructed to ibuprofen intercalated LDHs having different gallery heights, which indicated different intercalation capacities. Due to their mesoporosity these unique MMOs have particular potential as drug or catalyst carriers.

Crown Copyright © 2010 Published by Elsevier Inc. All rights reserved.

1. Introduction

Current needs in controlled release of therapeutic agents have triggered an intensive quest in the design of porous, especially hierarchical mesoporous materials. Carbon [1] and silica [2] nanofibers, Coesite [3], solid and hollow spheres [4,5], core–shell structured composites [6], poly(phenylenevinylene) networks [7], organosilica thin films [8], all exhibiting mesoporosity, have been synthesized in recent years. Periodic mesoporous structure imparts high specific surface area and pore volume. Moreover, the moderate channels (2–50 nm) favour the effective loading and delivery of drug molecules [9]. By the virtue of these advantages, many types of material, including inorganic silica, carbon, polymeric matrix and layered double hydroxides, will be more favourable for drug delivery, if a mesoporous nanostructure can be successfully assembled. Indeed, a series of surface-functionalized mesoporous silica nanoparticle materials, as efficient drug carriers, has been developed [10]. Despite their advantageous biocompatibility and interlayer anionic exchange capacity, only a few studies on the preparation of mesoporous layered double hydroxides have been reported [11].

Layered double hydroxides (LDHs) are well-known anionic or hydrotalcite-like clays with the general chemical formula $[M^{II}_{1-x}M^{III}_x(OH)_2]^{x+}[A^{n-}]_{x/n}\cdot mH_2O$, where M^{II} and M^{III} are divalent and trivalent cations and A^{n-} can be almost any organic or inorganic anion [12]. Their structure is based on $M^{2+}(OH)_6$ octahedral units sharing edges to build $M(OH)_2$ brucite-like layers. The positive layers and various intercalated anions attract enormous attention in the view of their vast applicability as drug and catalyst carriers [13,14], anticorrosion agents [15], absorbents [16] and modified electrode materials [17,18]. A number of synthetic routes, such as coprecipitation, ion-exchange, reconstruction and sol–gel process, have been employed in the preparation of LDHs [19]. When the LDHs are calcined at 400–500 °C, mixed metal oxides (MMOs) will be formed, along with the collapse of the LDHs layered structure. The production of MMOs cannot be achieved by ordinary mechanical means. Furthermore, they revert to their original layered structure when exposed to an alkaline solution. This so-called "memory effect" is usually used to intercalate large guests, such as amino acids and peptides [20], into the LDHs gallery.

It is difficult to create pores directly in the nano sized LDHs platelets; even the hierarchical pores of biotemplated LDHs, which have been obtained through the combination of atomic layer deposition (ALD) and a biotemplated synthesis technique [21], are not the channels in the LDHs sheets, but form part of their regular stack. However, Géraud et al. [22] and Halma et al. [23] have recently reported a general method to prepare three

* Corresponding author at: College of Material Science and Chemical Engineering, Harbin Engineering University, Harbin 150001, PR China.
Fax: +86 451 8253 3026.
E-mail address: zhqw1888@sohu.com (J. Wang).

0022-4596/$ - see front matter Crown Copyright © 2010 Published by Elsevier Inc. All rights reserved.
doi:10.1016/j.jssc.2010.08.027

dimensional ordered macroporous LDHs by using polystyrene crystal as template. Although the macropore diameter ranged from 300 to 500 nm, these studies render the possibility to induce formation of mesopores by a soft-template effect. Among various soft-templates, the structure directing behavior of Pluronic P123 ($(EO)_{20}(PO)_{70}(EO)_{20}$) [block PEO–PPO–PEO copolymer, PEO= poly(ethylene oxide), PPO=poly(propylene oxide)], a typical non-ionic surfactant has been widely used in the formation of mesoporosity [24,25]. In P123–water system, with P123 concentration increasing, different aggregates such as micelle, cubic, hexagonal and lamellar phases are formed [26]. Generally, after removal of P123 phase in precursor materials, the channel structure emerges. The removal process is often carried out by calcination or extraction with ethanol [27].

In this work, we describe the synthesis of Mg–Al layered double hydroxides by using P123 as a sacrifice template. After calcination of the as-synthesized LDHs, periodic mesoporous MMOs were obtained. By controlling the concentration of P123, we prepared a series of MMOs with different pore size distribution. Finally, ibuprofen (IBU) was used as a drug model to investigate the reconstruction of the mesoporous MMOs. The resulting LDHs and MMOs were characterized by XRD, SEM, TEM, FT-IR and N_2 adsorption–desorption measurement.

2. Experimental section

2.1. Materials

Pluronic P123 was purchased from Sigma-Aldrich, Inc. Ibuprofen was obtained from the General Pharmaceutical Factory of Harbin Pharmaceutical Group. Other inorganic reagents were purchased from Tianjin Kermel Chemical Reagents Development Center. All chemicals were of analytical grade and used without further purification.

2.2. Synthesis of the P123-templated LDHs and mesoporous MMOs

The precursor Mg–Al layered double hydroxides were synthesized through a coprecipitation process and hydrothermal treatment, in the presence of P123. NaOH solution was used as the precipitant. First, the precursor solution was prepared by dissolving 6.15 g (24.0 mmol) of $Mg(NO_3)_2\cdot 6H_2O$, 4.51 g (12.0 mmol) of $Al(NO_3)_3\cdot 9H_2O$ and a known weight of P123 in 60 mL of water. At 80 °C, the pH value of this solution was adjusted to 10.0 by addition of 2 mol/L NaOH. After vigorous stirring for 2 h, the formed suspension was transferred to an autoclave pressure vessel, and hydrothermally treated at 120 °C for 12 h. The resulting sol was washed with deionized water several times, and dried under vacuum at 80 °C for 24 h. The whole procedure was repeated, altering the amount of P123 added while keeping other reaction conditions constant, to obtain a series of P123-templated LDHs. The P123/water mass ratios were 0, 0.5, 1, 2, 5 and 10 wt%. Powder obtained from above process was calcined in air at 500 °C for 5 h in order to remove the template. The final resultant products were MMOs.

2.3. Recovery of MMOs to ibuprofen intercalated LDHs

The recovery of MMOs was carried out by the reconstruction method described as follows: a total of 0.5 g of Mg–Al MMOs was added to a solution of 1.04 g of IBU in 100 mL ethanol/water (1:1, volume). At 45 °C, the solution was brought to pH=10.0 by the addition of NaOH (2 mol/L) and then put in a thermostat shaking water bath for 24 h. The solid product was washed with water and ethanol, and then dried in a vacuum oven at 80 °C for 24 h. The IBU intercalated LDHs prepared by this method was abbreviated here as Mg_2Al–$(IBU)_{re}$.

2.4. Calibration graphs for ibuprofen determination

Calibration graph of absorbance versus concentration of the free ibuprofen was plotted by monitoring the ibuprofen typical UV absorption band at 264 nm for a concentration range 20–400 μg/mL of the drug in the mixture of 1:1 (v/v) ethanol −1 mol/L HCl. The amount of ibuprofen intercalated in the LDH gallery was determined by comparing the absorbance of sample solution to the data from calibration curve.

2.5. Characterizations

Powder X-ray diffraction (XRD) patterns of the solid products were obtained in the 2θ range of 5–75° using a Rigaku D/max-IIIB diffractometer with Cu–$K\alpha$ radiation (λ=1.54178 Å). Morphology was characterized using transmission electron microscopy (TEM, PHILIPS CM 200 FEG, 160 kV), and scanning electron microscope (SEM, JEOL JSM-6480A microscope). Fourier-transform infrared (FT-IR) spectrum was recorded with an AVATAR 360 FT-IR spectrophotometer using a standard KBr pellet technique. The textural properties of the MMOs were determined by nitrogen adsorption at 77 K using a Micromeritics ASAP2010 setup.

3. Results and discussion

The XRD patterns of P123-templated Mg–Al LDHs, mesoporous MMOs, and the standard data for carbonate intercalated Mg–Al LDHs are displayed in Fig. 1. For P123-templated LDHs (Fig. 1a), the broadband at 2θ=23° can be assigned to the amorphous P123 residual in LDHs structure. Two shoulder bands at 18.5° and 20.5° are assigned to $Al(OH)_3$ phase. The other diffraction peaks can be readily indexed to a hexagonal lattice ($R\bar{3}m$ space group) of carbonate intercalated Mg–Al LDHs. The emergence of additional $Al(OH)_3$ suggests that the template P123 may restrain the growth of Mg–Al LDHs to some extent. In other words, both P123 and $Al(OH)_3$ participated in the formation of micelles. This is also the reason that the as-synthesized Mg–Al LDHs solution became sol after hydrothermal treatment. In order to create ordered mesopores, the copolymer surfactant P123 was removed by employing a calcination process at 500 °C, instead of using ethanol

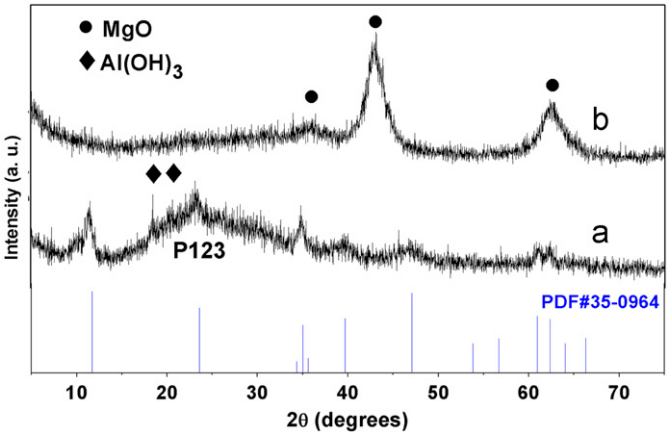

Fig. 1. XRD patterns of P123-templated Mg–Al LDHs (a), mesoporous MMOs (b), and the standard data for carbonate intercalated Mg–Al LDHs (PDF no. 35-0964). The amount of P123 is 2 wt%.

as extracting agent [28]. During calcination, the P123-templated Mg–Al LDHs underwent complicated thermal decompositions, which have been reported in literature [29,30]. In Fig. 1b, after removal of P123, three evident peaks ascribed to (111), (200) and (220) of MgO (PDF no. 65-0476) are well defined with no other detectable crystal phase, indicating the mesoporous MMOs is cubic MgO doped with amorphous Al_2O_3 species. It should be noted that the heated temperature of P123-templated LDHs is best not to exceed 600 °C because at these higher temperatures, Mg–Al MMOs will convert to $MgAl_2O_4$ spinel and δ–Al_2O_3, resulting in an irrecoverable LDHs layered structure [31].

The FT-IR spectra illustrated in Fig. 2 also demonstrate the changes between P123-templated LDHs and mesoporous MMOs. In Fig. 2a and b, the peaks at 2970, 2932 and 2878 cm^{-1} are attributed to the alkyl stretching vibrations and peaks at 1108 cm^{-1} are attributed to C–O stretching vibrations [32]. Both of these indicate the presence of P123 in as-synthesized Mg–Al LDHs. In Fig. 2b and c, the feature peaks of Mg–Al LDHs can be observed, including a wide band at 3465 cm^{-1} (ν_{OH}), a shoulder at 3122 cm^{-1} (ν_{OH} for O–H bond H–bound with CO_3^{2-}), a weak band at 1637 cm^{-1} [$\delta(H_2O)$ corresponding to water deformation], and a strong peak at around 1385 cm^{-1} [due to $\nu(CO_3^{2-})$] [33,34]. These data are in accord with the results from XRD analysis. In reality, the FT-IR spectrum in Fig. 2c should be assigned to carbonate intercalated Mg–Al LDHs, because of the re-hydration effect [22,35] during the preparation of MMOs–KBr pellet.

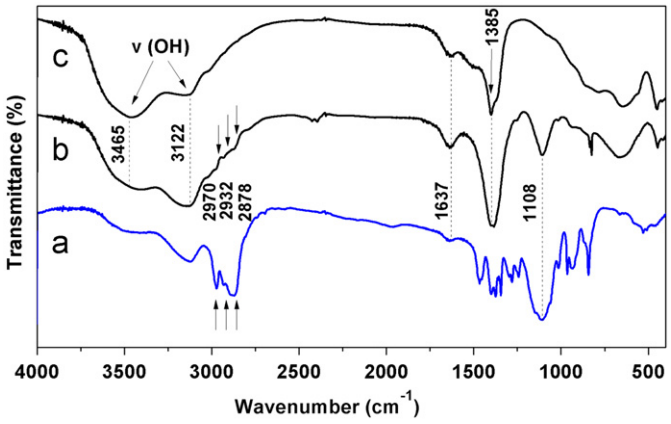

Fig. 2. FT-IR spectra for P123 (a), P123-templated Mg–Al LDHs (b) and mesoporous MMOs (c). The amount of P123 is 2 wt%.

The morphologies of the products are examined by SEM and TEM, as shown in Fig. 3. It can be seen that all the particle sizes of LDHs are about 2–3 μm (Fig. 3a), and the plate-like LDHs sheets are stacked perpendicularly on the surface (Fig. 3b). The aggregation is similar to the LDHs prepared by the urea hydrolysis method in sodium dodecanesulfonate aqueous solution [36]. The formation of LDHs aggregate morphology starts from the aggregate of $Al(OH)_3$ and P123, and, following hydrothermal treatment, Mg^{2+} is precipitated and LDHs sheets are formed. The P123 molecules dispersed in the LDHs kept stable during the nucleation and crystal growth. Fig. 3c shows that the MMOs based on the calcination of P123-templated Mg–Al LDHs appears like irregular grains, with a size distribution of 50–100 nm. The ordered mesopore structure of MMOs, with pore diameter about 2.2 nm, is clearly evident from the HRTEM (Fig. 3d). In our experiment, we also expected to obtain mesoporous Mg–Al LDHs by direct removal of P123 using ethanol as extractant. The resulting pore diameter, however, was smaller than 2.2 nm (see Figure S1 in Supporting Information). This enlargement of MMOs pores could be due to the thermal contraction and decomposition of Mg–Al LDHs.

The typical N_2 adsorption–desorption isotherms and pore size distributions of MMOs samples are presented in Fig. 4,

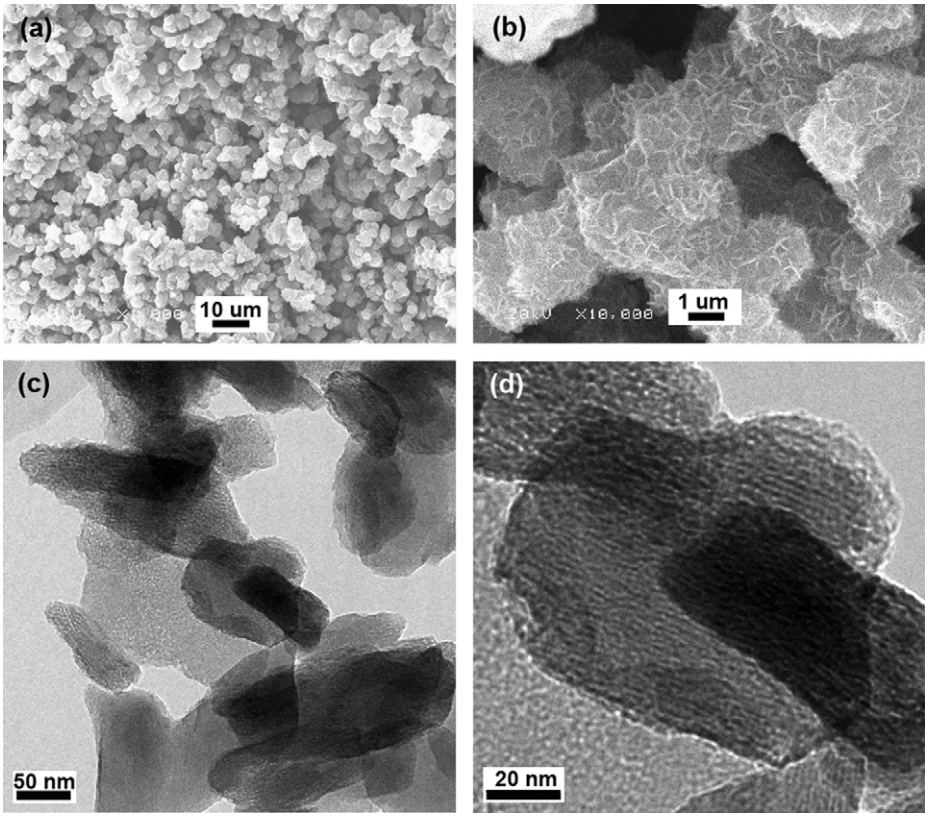

Fig. 3. SEM images of P123-templated Mg–Al LDHs (a, b) and TEM images of mesoporous MMOs (c, d). The amount of P123 is 2 wt%.

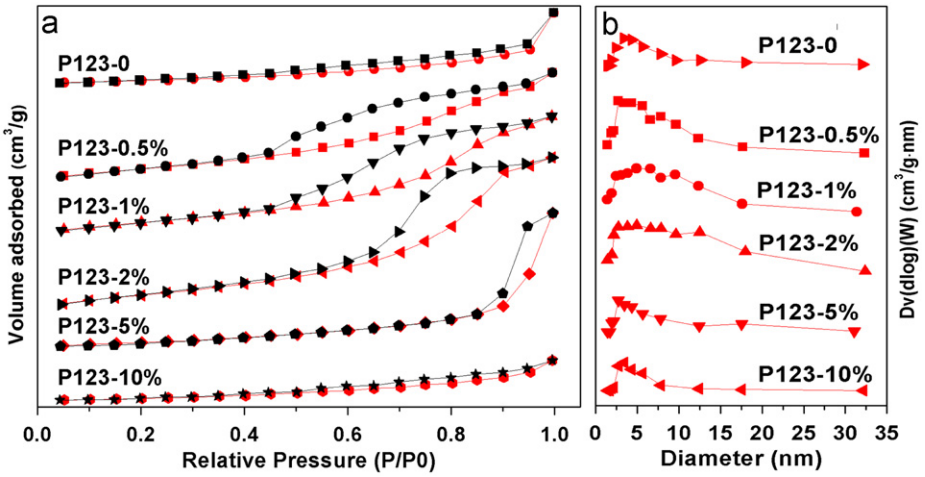

Fig. 4. N_2 adsorption–desorption isotherms (a) and pore size distributions (b) of MMOs synthesized under different P123/water mass ratio: 0, 0.5, 1, 2, 5 and 10 wt%.

Table 1
Specific surface areas and pore parameters of MMOs synthesized with different amounts of P123.

P123/water mass ratio	0	0.5 wt%	1 wt%	2 wt%	5 wt%	10 wt%
S_{BET} (m^2/g)[a]	17.9	85	92.3	108.1	30.7	13.5
V_P (cm^3/g)[b]	0.114	0.190	0.204	0.249	0.206	0.073
d_P (nm)[b]	3.82	3.82	3.82	7.74	2.74	2.43

[a] Performed by multipoint BET method.
[b] Cumulative desorption pore volume and average pore diameter performed by BJH method.

and the corresponding textural data are compiled in Table 1. The MMOs prepared without P123, exhibits a minor hysteresis loop ($P/P_0 > 0.4$) and a rapid adsorption at higher P/P_0, implying mainly the presence of macropores [37]. The MMOs, synthesized with P123/water mass ratio of 0.5, 1 and 2 wt%, exhibit a typical *IV* isotherm with a H3-type hysteresis loop ($P/P_0 > 0.4$), implying the presence of mesopores [38]. In addition, the limiting adsorption at higher P/P_0 indicates the disappearance of macropores compared to MMOs prepared without P123. However, the increase of P123 concentration restricts the formation of mesoporosity rather than improving the mesoporous structure of MMOs. The hysteresis loop shifts to a higher pressure, between 0.85 and 1.0, when the P123/water mass ratio is 5 wt%. Moreover, the higher concentration (10 wt%) of P123 almost leads to the overlapping of adsorption and desorption curves, which indicates that the corresponding MMOs have less mesopores. These results are further confirmed by the pore size distribution in Fig. 4b. The MMOs sample synthesized with 2 wt% P123 has a wider distribution (2–18 nm, maximum at 4.8 nm) of pore size than other samples, and its average pore diameter (7.74 nm) is also larger than that of others.

To investigate the effect of mesopores on preparing LDHs by the reconstruction method, the MMOs synthesized with 2 wt% P123 and without P123 were used as precursors to recover IBU intercalated LDHs. The resulting XRD patterns are shown in Fig. 5. Fig. 5a shows the XRD pattern of carbonate intercalated LDHs prepared by coprecipitation without P123. The (003), (006) and (012) diffraction peaks, which correspond to the basal and higher order reflections, appear at 11.7, 23.4 and 34.5, respectively. The calculated basal spacing d_{003} is 0.765 nm. The first diffraction peaks observed from both reconstructed LDHs can be ascribed to the (003) reflection of IBU intercalated LDHs, resulting in a basal spacing (d_{003}) of about 3.12 (Fig. 5b) and 1.19 nm (Fig. 5c). The different values of d_{003}

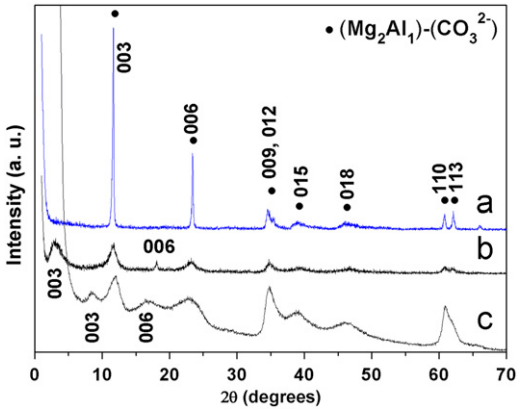

Fig. 5. XRD patterns of Mg_2Al–$(CO_3^{2-})_{cop}$ (a) and Mg_2Al–$(IBU)_{re}$ based on MMOs synthesized with 2 wt% P123 (b) and without P123 (c), respectively.

derive from the different orientation (see Fig. 6) of IBU molecule in the LDHs gallery. It is reported in literature [39] that IBU is difficult to intercalate into LDHs through the reconstruction method because of the competition of hydroxide and carbonate. Nevertheless, the mesopores in the MMOs provide channels to adsorb IBU molecules which are finally intercalated between LDHs layers. Assuming a thickness of 0.48 nm for LDHs layer, the gallery heights for both Mg_2Al–$(IBU)_{re}$ are about 2.74 (Fig. 5b) and 0.71 nm (Fig. 5c). Considering the width and length of the IBU molecule, are 0.52 and 1.03 nm [40], the calculated gallery heights suggest a bilayer and a monolayer arrangement of the intercalated IBU as shown in Fig. 6. Meanwhile, the UV-measured IBU loading amount for the Mg_2Al–$(IBU)_{re}$ synthesized with 2 wt% P123 is 35.4% (w/w); but for the Mg_2Al–$(IBU)_{re}$ synthesized without P123, the amount is only 20.6% (w/w). Therefore, the design of mesopores in MMOs not only offers a higher specific surface area but also enhances its intercalation capacity with IBU by the reconstruction method. The FT-IR spectra and ibuprofen release profiles of the above MgAl–$(IBU)_{re}$ can be found in Figure S2 and Figure S3 in Supporting Information.

4. Conclusion

In this paper, using a P123-assisted hydrothermal method, we synthesized P123-templated Mg–Al LDHs. The mesoporous MMOs were obtained after removal of P123. The effect of P123 amounts on the textural structure of MMOs was investigated by

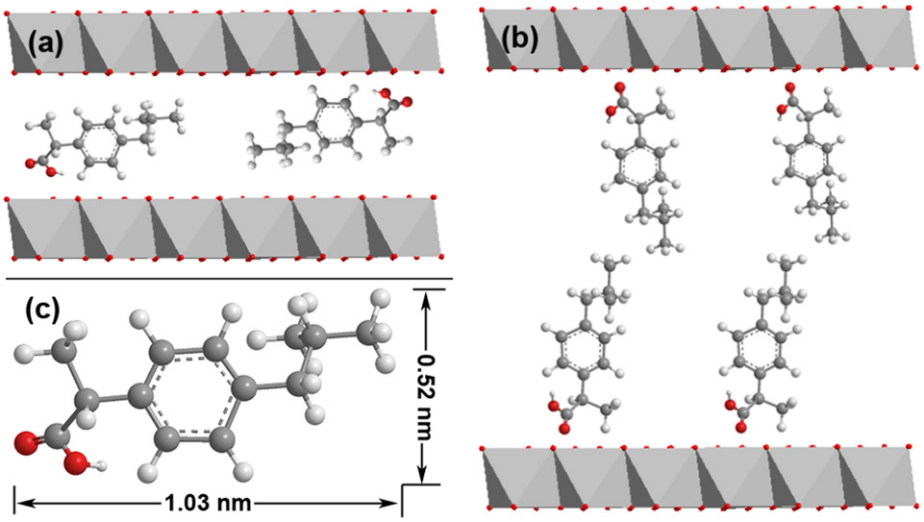

Fig. 6. Structural models of Mg_2Al–$(IBU)_{re}$: (a) monolayer and (b) bilayer intercalation, and IBU molecule (c).

N_2 adsorption–desorption, and the results indicated that when P123 concentration was 2 wt%, the mesoporous MMOs exhibited higher specific surface area and wider distribution of pore size. Through the reconstruction method, the MMOs fabricated with 2 wt% P123 and without P123 converted to IBU intercalated LDHs in the presence of IBU. The XRD analysis revealed the different molecular orientation of intercalated ibuprofen, due to the mesoporous structure of MMOs.

Acknowledgment

This work was supported by the Key Project of Chinese Ministry of Education, Special Innovation Talents of Harbin Science and Technology (2010RFXXG007), Fundamental Research Funds for the Central University (HEUCF101010) and China Postdoctoral Science Foundation (AUGA41309003).

Appendix A. Supplementary material

Supplementary data associated with this article can be found in the online version at doi:10.1016/j.jssc.2010.08.027.

References

[1] G. Zhao, J. He, C. Zhang, J. Zhou, X. Chen, T. Wang, J. Phys. Chem. C 112 (2008) 1028.
[2] L. Zhou, G. Hong, L. Qi, Y. Lu, Langmuir 25 (2009) 6040.
[3] P. Mohanty, Y. Fei, K. Landskron, J. Am. Chem. Soc. 131 (2009) 9638.
[4] S.Z. Qiao, C.X. Lin, Y. Jin, Z. Li, Z. Yan, Z. Hao, Y. Huang, G.Q. Lu, J. Phys. Chem. C 113 (2009) 8673.
[5] S. Huang, Y. Fan, Z. Cheng, D. Kong, P. Yang, Z. Quan, C. Zhang, J. Lin, J. Phys. Chem. C 113 (2009) 1775.
[6] P. Yang, Z. Quan, Z. Hou, C. Li, X. Kang, Z. Cheng, J. Lin, Biomaterials 30 (2009) 4786.
[7] Ro Dawson, F. Su, H. Niu, C.D. Wood, J.T.A. Jones, Y.Z. Khimyak, A.I. Cooper, Macromolecules 41 (2008) 1591.
[8] M.A Wahab, H. Hussain, C. He, Langmuir 25 (2009) 4743.
[9] S. Wang, Microporous Mesoporous Mater 117 (2009) 1.
[10] I.I. Slowing, J.L. Vivero-Escoto, C.W. Wu, V.S.Y. Lin, Adv. Drug Delivery Rev. 60 (2008) 1278.
[11] Z.A. Hu, Y.L. Xie, Y.X. Wang, H.Y. Wu, Y.Y. Yang, Z.Y. Zhang, Electrochim. Acta 54 (2009) 2737.
[12] J.S. Valente, M. Sànchez-Cantù, E. Lima, F. Figueras, Chem. Mater. 21 (2009) 5809.
[13] H.S. Panda, R. Srivastava, D. Bahadur, J. Phys. Chem. B 113 (2009) 15090.
[14] C. Resini, T. Montanari, L. Barattini, G. Ramis, G. Busca, S. Presto, P. Riani, R. Marazza, M. Sisani, Fa Marmottini, U. Costantino, Appl. Catal. A355 (2009) 83.
[15] S.K. Poznyak, J. Tedim, L.M. Rodrigues, A.N. Salak, M.L. Zheludkevich, L.F.P. Dick, M.G.S. Ferreira, Appl. Mater. Interfaces 1 (2009) 2353.
[16] T.W. Kim, M. Sahimi, T.T. Tsotsis, Ind. Eng. Chem. Res. 48 (2009) 5794.
[17] J. Qiu, G. Villemure, J. Electroanal. Chem. 395 (1995) 159.
[18] M. Li, F. Ni, Y. Wang, S. Xu, D. Zhang, L. Wang, Appl. Clay Sci. 46 (2009) 396.
[19] J. He, M. Wei, B. Li, Y. Kang, D.G. Evans, X. Duan, Struct. Bond 119 (2006) 89.
[20] H. Nakayama, N. Wada, M. Tsuhako, Int. J. Pharm. 269 (2004) 469.
[21] Y. Zhao, M. Wei, J. Lu, Z.L. Wang, X. Duan, ACS Nano 3 (2009) 4009.
[22] E. Géraud, V. Prévot, J. Ghanbaja, F. Leroux, Chem. Mater. 18 (2006) 238.
[23] M. Halma, K.A.D.F. Castro, V. Prévot, C. Forano, F. Wypych, S. Nakagaki, J. Mol. Catal. A: Chem. 310 (2009) 42.
[24] X. Li, X. Wang, H. Chen, P. Jiang, X. Dong, J. Shi, Chem. Mater. 19 (2007) 4322.
[25] M.A.U. Martines, E. Yeong, A. Larbot, E. Prouzet, Microporous Mesoporous Mater 74 (2004) 213.
[26] Y. Zhao, X. Chen, C. Yang, G. Zhang, J. Phys. Chem. B 111 (2007) 13937.
[27] A. López-Noriega, E. Ruiz-Hernández, S.M. Stevens, D. Arcos, M.W. Anderson, O. Terasaki, M. Vallet-Regí, Chem. Mater. 21 (2009) 18.
[28] X. Guo, H. Guo, L. Fu, R. Deng, W. Chen, J. Feng, S. Dang, H. Zhang, J. Phys. Chem. C 113 (2009) 2603.
[29] H. Zhang, S.H. Guo, K. Zou, X. Duan, Mater. Res. Bull. 44 (2009) 1062.
[30] S.K. Sharma, P.A. Parikh, R.V. Jasra, J. Mol. Catal. A: Chem. 301 (2009) 31.
[31] A.J. Marchi, C.R. Apesteguía, Appl. Clay Sci. 13 (1998) 35.
[32] A.F. Demirörs, B.E. Eser, Ö. Dag, Langmuir 21 (2005) 4156.
[33] Z.P. Xu, N.D. Kurniawan, P.F. Bartlett, G.Q. Lu, Chem. Eur. J. 13 (2007) 2824.
[34] F. Li, X. Jiang, D.G. Evans, X. Duan, J. Porous Mater. 12 (2005) 55.
[35] T. Stanimirova, T. Hibino, V. Balek., J. Therm. Anal. Calorim. 84 (2006) 473.
[36] B. Li, J. He, J. Phys. Chem. C 112 (2008) 10909.
[37] L. Zhou, W. Wang, H. Xu, S. Sun, M. Shang, Chem. Eur. J. 15 (2009) 1776.
[38] R.M. Grudzien, S. Pikus, M. Jaroniec, J. Phys. Chem. C 113 (2009) 4875.
[39] C.R. Gordijo, C.A.S. Barbosa, A.M.D.C. Ferreira, V.R.L. Constantino, D.D.O. Silva, J. Pharm. Sci. 94 (2005) 1135.
[40] M. Vallet-Regi, A. Rámila, R.P. Real, J. Pérez-Pariente, Chem. Mater. 13 (2001) 308.